Proc. Indian Acad. Sci. (*Chem. Sci.*), Vol. 115, Nos 5 & 6, October–December 2003, pp 637–647

Aromaticity in benzene-like rings – An experimental electron density investigation¶

ANUPAMA RANGANATHAN and G U KULKARNI*
Chemistry and Physics of Materials Unit, Jawaharlal Nehru Centre for Advanced Scientific Research, Jakkur PO, Bangalore 560 064, India
e-mail: kulkarni@jncasr.ac.in

Abstract. An experimental charge density study has been carried out on perylene based on X-ray diffraction measurements at 130 K. The electron density and its associated properties have been evaluated at the bond and the ring critical points for the naphthalene residues as well as for the central ring. The variation of the Laplacian along the axis, above and below the ring plane, is found to be symmetric for the central ring while for the naphthalene rings, the Laplacian values are enhanced under the bow-shaped region. A plot of the Laplacian versus density evaluated at various points along the axis above the ring plane, shows a steep variation in the case of the central ring implying that the *p*-density is smeared out compared to that over the naphthalene rings. Similar data extracted from a quinoid ring and a regular phenyl ring (both based on earlier reports from this laboratory) exhibit increasingly shallower trends and indicate, by contrast, that the central ring of perylene is much less aromatic.

Keywords. Perylene; aromaticity; experimental electron density.

1. Introduction

The concept of aromaticity in cyclic systems has been widely studied employing a multitude of experimental and theoretical methods.[1] Experimental methods include spectroscopic techniques such as NMR,[2] X-ray crystallography and magnetic measurements,[3] while theoretical approaches mainly pertain to resonance energy calculations[4] and graph-topological evaluations.[5] Although there are a number of reports on molecular orbital based descriptions of aromaticity,[6] surprisingly, little attention has been paid to the relationship between the topological characteristics of the charge distribution and the aromatic character, particularly in relation to the conjugated p-electron framework. Studies that deal with electron density properties at the bond critical points in cyclic molecules do not really suffice to provide a consistent description of aromaticity.[7] Howard and Krygowski,[8] in their theoretical study of benzenoid hydrocarbons, emphasized the importance of the charge density parameters evaluated at the ring critical point (RCP) in describing the aromatic character of a molecule.

In a previous study on oxocarbon dianions,[9] we analysed the charge density distribution in the rings in relation to their p-electron delocalisation, using the electron density and its curvatures at the RCP. Indeed, a plot of the Laplacian versus the electron density evaluated at the RCP (see figure 1), for a number of cyclic systems revealed a major

¶Dedicated to Professor C N R Rao on his 70th birthday
*For correspondence

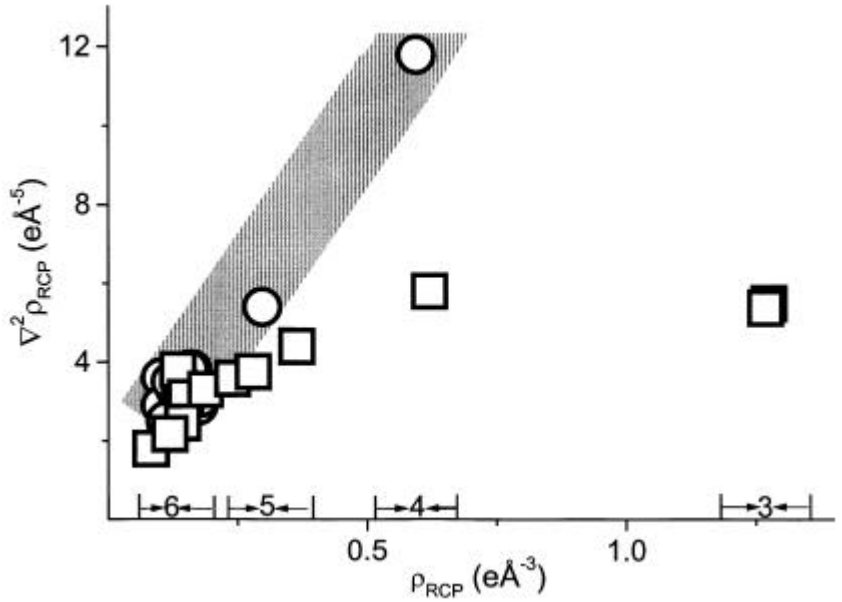

Figure 1. Plot of Laplacian versus electron density for *n*-membered cyclic systems (n = 3, 4, 5, 6). Circles depict aromatic rings and squares, the non-aromatic rings. The hashed region is where the Laplacian varies proportional to the electron density. The numbers over the *x*-axis denote the size of the ring. The description of the data points is given in ref. [9].

difference in the trends exhibited by the aromatic and the nonaromatic rings. It was noted that all the aromatic rings of different ring sizes fall in a narrow band, where the Laplacian varies nearly proportional to the density, while the nonaromatic rings showed no systematic trend. For small, three- and four-membered rings, the distinction is quite clear. In the case of six-membered rings, however, the aromatic and nonaromatic ring points appear clustered in a region of low density and Laplacian. The plot in figure 1 is therefore, less helpful in such situations. The present study is an attempt to resolve this difficulty.

The molecule chosen for this study is perylene (the first member of the perylene-terrylene-quaterrylene series), a polycyclic aromatic hydrocarbon with two naphthalene residues giving rise to four fused rings and a central ring, the latter formed by the *peri*-bonds. Perylene derivatives are commercially used in photovoltaics and automotive paints.[10] A previous report[11] on its crystal structure had raised questions on the aromatic nature of the central ring. Is aromaticity restricted to only the naphthalene residues? How aromatic is the central ring? Our interest was to investigate these aspects using the experimental charge density method based on X-ray crystallography. The study was extended to a quinoid ring that exists in 7,7-di[(*S*)-(+)-2-(methoxymethyl)pyrrolidino]-8,8-dicyanoquinodimethane (DMPDQ),[12] a molecule known for its nonlinear optical properties. Comparisons have also been made with a regular phenyl ring in *N*-methyl-*N*-(2-nitrophenyl) cinnamanilide.[13] The study has indeed provided a means of evaluating aromaticity in benzene-like rings.

2. Experimental

Commercially available perylene (Fluka) was recrystallised from a benzene solution by slow evaporation at room temperature. Yellowish orange plate-like crystals were obtained. A good quality single crystal of the compound was chosen after examination under an optical microscope. X-ray diffraction intensities were measured by ω scans using a Siemens three-circle diffractometer attached with a CCD area detector and a graphite monochromator for the MoKα radiation (50 kV, 40 mA). The crystals were cooled to 130 K on the diffractometer using a stream of cold nitrogen gas from a vertical nozzle and the temperature was maintained within 1 K throughout the data collection.

The unit cell parameters and the orientation matrix of the crystal were initially determined using ~45 reflections from 25 frames collected over a small ω scan of 7·5° sliced at 0·3° interval. A hemisphere of intensity data of the reciprocal space with 2θ settings of the detector at 28° and 70° was collected. Data reduction was performed using the SAINT program (Siemens, USA, 1995) and the orientation matrix along with the detector and the cell parameters were refined for every 40 frames on all the measured reflections. The crystal structures were first determined with the low-resolution data up to $\sin\theta/\lambda = 0{\cdot}56$ Å^{-1}. Absorption correction was applied for both the systems using the SADABS program (Siemens, USA, 1995). The phase problem was solved by direct methods and the non-hydrogen atoms were refined anisotropically, by means of the full-matrix least-squares procedure using the SHELXTL program (Siemens, USA, 1995). All the hydrogen atoms were located using the difference Fourier method. Crystal structure parameters have been deposited at CCDC number 215338. The crystal structure of perylene has been reported by a few workers,[11,14] while the charge density data on this molecule is reported for the first time by us.

Charge density analysis was carried out based on multipole expansion of the electron density centred at the nucleus of the atom. Accordingly, the aspherical atomic density can be described in terms of spherical harmonics,[15]

$$\rho_{\text{atom}}(r) = \rho_{\text{core}}(r) + \rho_{\text{valence}}(r) + \rho_{\text{def}}(r).$$

Thus for each atom,

$$\rho_{\text{atom}}(r) = \rho_{\text{core}}(r) + P_v \kappa^3 \rho_{\text{valence}}(\kappa r) + \sum_{l=0} \kappa'^3 R_l(\kappa' r) \sum_{m=0} \sum_{p=\pm l} P_{\text{lmp}} Y_{\text{lmp}}(\theta, \phi),$$

with the origin at the atomic nucleus. The population coefficients, P_{lmp}, are to be refined along with the κ and κ' parameters which control the radial dependence of the valence shell density. The analysis was carried out in several steps.

The H atom positions were found using the difference Fourier method and were adjusted to average neutron values[16] as commonly done during the multipole refinement (normalized X-ray geometries, C(ar)–H, 1·085 Å). A high order refinement of the data was performed using reflections with $\sin\theta/\lambda \geq 0{\cdot}6$ Å^{-1} and $F_o \geq 4\sigma$. All the hydrogens were held constant throughout the refinement along with their isotropic temperature factors. Multipolar refinement for the charge density analysis was carried out using the XDLSM routine of the XD package[17] and the details are given in table 1. The atomic coordinates and the thermal parameters obtained from the high-order refinement were

used as input to XD refinement. The carbon atoms were refined up to octapole while hydrogens were truncated at dipole. The charge neutrality constraint was applied to the asymmetric unit. Kappa refinement was carried out on both the spherical and deformation valence shells of the carbon atoms while those for the hydrogen atoms were restricted to the spherical valence. The multipolar refinement strategy was the following: (a) scale

Table 1. Crystal structure data of perylene.

Chemical formula	$C_{20}H_{12}$
Formula weight	252·30
Cell setting	Monoclinic
Space group	$P2_1/c$
a (Å)	9·7450(1)
b (Å)	5·8232 (1)
c (Å)	10.5824 (1)
a (°)	90
b (°)	107·452 (1)
g (°)	90
r (kg/m^3)	1·405
m, mm^{-1}	0·080
Cell volume (Å^3)	596·43 (1)
Crystal size (mm)	0·40 × 0·30 × 0·35
Z	2
F(000)	264
Diffractometer	Siemens CCD 3 circle diffractometer
Radiation type	MoK_a (0·71073 Å)
Crystal-detector distance (cm)	5·0
Temperature (K)	130 (2)
No. of measured reflections	9862
No. of independent reflections	4891
R_{merge}	0·064
R_{int}	0·038
q_{max} in q/l (Å^{-1})	49·44, 1·07
Range of h, k, l	$-20 \le h \le 20$ $-12 \le k \le 10$ $-21 \le l \le 14$
Refinement	
Refinement on F^2	
R_1	0·071
WR_2	0·193
S	0·953
No. of reflections used in the refinement	4891
No. of parameters refined	115
After multipole refinement	
Weighting scheme	0·087, 0·143
$R\{F\}$	0·044
$R\{F^2\}$	0·067
S	1·084
No. of variables	274
N_{ref}/N_v	14·5
Cambridge crystallographic database deposition number	CCDC 215338

factor, (b) P_V, (c) P_{1mp} (steps b and c until convergence). (d) κ, (e) steps b and c until convergence, (f) κ', (g) steps b and c until convergence, (h) positional and thermal parameters of all the non-hydrogen atoms, and finally (i) P_V and P_{1mp} together. Difference mean square displacement amplitudes (DMSDA) for the various bonds obtained from XD were found to follow the Hirshfeld criterion closely.[18] The quality of the refinement was monitored by observing the residuals as well as the residual maps. The latter were found to be featureless in different planes of the molecule.

The important bond parameters are the total density at the bond critical point (ρ_{BCP}) and its Laplacian, $\nabla^2\rho_{BCP}$, which is the arithmetic sum of the three eigenvalues ($\lambda_1 + \lambda_2 + \lambda_3$) along the principal axes. The XDPROP routine was used to calculate these quantities. The routine was also used to calculate properties at the ring critical points. The static deformation density (total density – promolecular density) maps have been plotted using the XDGRAPH routine. The crystallographic data, geometrical and charge density parameters are listed in tables 1–3. Such details for the quinoid compound, DMPDQ[12] and for the cinnamanilide derivative[13] have been earlier reported from this laboratory.

3. Results and discussion

Perylene crystallizes in a monoclinic, $P2_1/c$ space group. The asymmetric unit, shown in figure 2, consists of only a part of the molecule, the rest of the atoms are related by centre

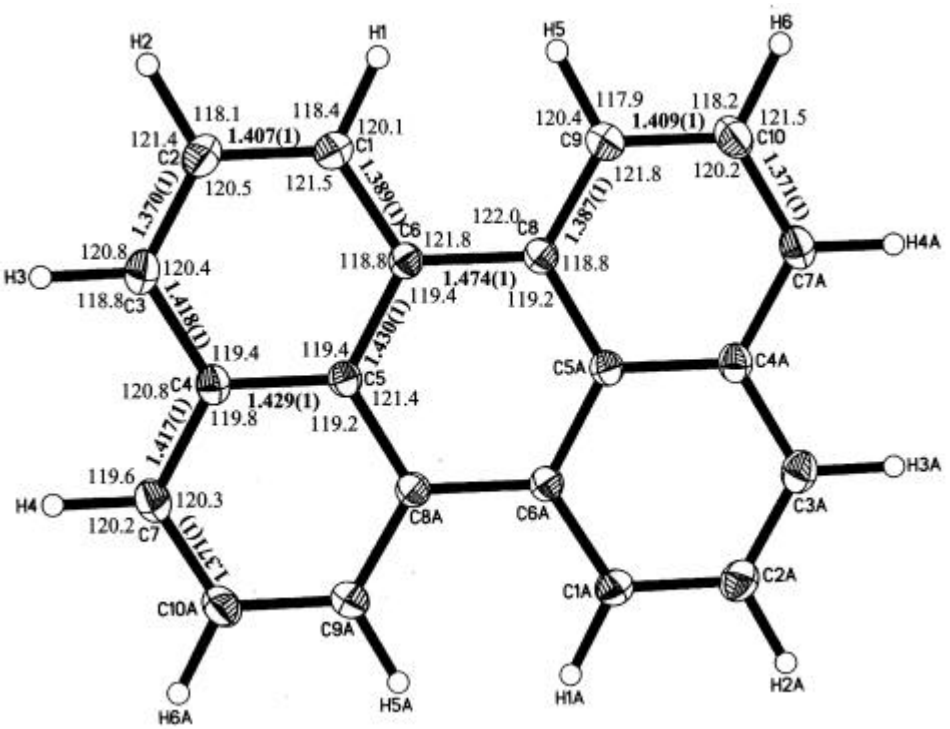

Figure 2. ORTEP diagram of perylene. Thermal ellipsoids are shown at 50% probability. The bond lengths and the angles are shown for the asymmetric unit.

Table 2. Torsional angles in perylene.

Moiety	Torsion angle (°)	Moiety	Torsion angle (°)
C6–C1–C2–C3	0·05	C4–C7–C10–C9	0·79
C2–C1–C6–C5	−0·53	C5–C8–C9–C10	0·16
C2–C1–C6–C8A	180·00	C6A–C8–C9–C10	−179·86
C1–C2–C3–C4	0·43	C8–C9–C10–C7	−0·55
C2–C3–C4–C5	−0·43	C6–C1–C2–H2	−179·00
C2–C3–C4–C7	179·13	H1–C1–C2–C3	178·80
C3–C4–C5–C6	−0·05	H1–C1–C2–H2	−0·25
C3–C4–C5–C8	179·84	H1–C1–C6–C5	−179·25
C7–C4–C5–C6	−179·61	H1–C1–C6–C8A	1·27
C7–C4–C5–C8	0·27	C1–C2–C3–H3	−179·20
C3–C4–C7–C10	179·78	H2–C2–C3–C4	179·45
C5–C4–C7–C10	−0·66	H2–C2–C3–H3	−0·19
C4–C5–C6–C1	0·52	H3–C3–C4–C5	179·22
C4–C5–C6–C8A	−180·00	H3–C3–C4–C7	−1·22
C8–C5–C6–C1	−179·37	C3–C4–C7–H4	1·25
C8–C5–C6–C8A	0·12	C5–C4–C7–H4	−179·19
C4–C5–C8–C9	−0·03	C4–C7–C10–H6	178·09
C4–C5–C8–C6A	179·98	H4–C7–C10–C9	179·32
C6–C5–C8–C9	179·85	H4–C7–C10–H6	−3·39
C6–C5–C8–C6A	−0·13	C5–C8–C9–H5	−179·11
C1–C6–C8A–C5A	179·36	C6A–C8–C9–H5	0·87
C1–C6–C8A–C9A	−0·66	C8–C9–C10–H6	−177·93
C5–C6–C8A–C5A	−0·12	H5–C9–C10–C7	178·73
C5–C6–C8A–C9A	179·86	H5–C9–C10–H6	1·35

of symmetry. The bond lengths and valence angles of the ring C–C bonds are also indicated in this figure. All the C–C distances are in the range of 1·41–1·43 Å, except the *peri*-bonds (C6–C8 and C6A–C8A), which are somewhat longer, 1·474(1) Å, the value being closer to the sp^2–sp^2 single bond distance of 1·48 Å[19] but considerably shorter than the sp^3–sp^3 value of 1·54 Å. The measured *peri*-bond distances are in good agreement with the reported values.[11] This suggests that the benzenoid character in perylene is probably not completely localised in the naphthalene residues, but tends to spread over the whole molecule. The inner C–C bond distances (C4–C5, 1·429(1) Å and C5–C6, 1·430(1) Å) are considerably longer than the outer bonds (C2–C3, 1·370(1) Å and C7–C10A, 1·371(1) Å). The C–H distances are ~1·08 Å. The C–C–C valence angles are in the range 120°–122°, while the C–C–H angles are ~118°–120°. The five rings are not in a perfect planar arrangement; there are small, but significant deviations from planarity, the magnitude of the deviations from the mean plane varying from ~1° to 3·4° (see table 2). As a result, the molecule is slightly bow-shaped.[11] The structure is largely stabilized by herringbone-like interactions between the naphthalene residues, the intermolecular separations being ~3·45 Å.

The next step in our analysis was to derive the electron densities ($\boldsymbol{r}(r)$) and the derivatives of $\boldsymbol{r}(r)$ for all the bonds in perylene. Figure 3 depicts the static deformation density maps of the five rings in perylene. Concentric contours typify the various bonding regions in the molecule between the atom-cores. The C–C bonding density in the rings appears uniform across the internuclear axes. The values of the electron density and the

Laplacian at the bond critical point for the bonds forming the two naphthalene residues are in the range: 1·90–2·40 eÅ^{-3} and −17·1 to −24 eÅ^{-5}, respectively. The *peri*-bonds (C6–C8 and C6A–C8A) forming the central ring have slightly lower densities and Laplacians (1·78(4) eÅ^{-3} and −12·0(1) eÅ^{-5}). The dominant, perpendicular curvatures (λ_1 and λ_2) for the *peri*-bonds are also smaller (~−15 and −10·5 eÅ^{-5}, respectively) in comparison to those associated with the two naphthalene residues (~−20 and −15 eÅ^{-5}, see table 3). In comparison to the C–C bonds, the C–H bonds exhibit significantly lower ρ and $\nabla^2\rho$ values at their BCPs (~1.7 eÅ^{-3} and ~−12 eÅ^{-5}).

As mentioned earlier, it is of interest to see how the charge density descriptors at the ring critical point (RCP) may be useful in describing aromaticity of the rings. For this purpose, we have analysed the RCP properties of the five rings forming perylene. The two phenyl rings in each naphthalene residue exhibit slightly different values of density (~0·09 and ~0·11 eÅ^{-3}), but similar Laplacian values (~2·4 eÅ^{-5}). The central ring exhibits density and Laplacian values of 0·096(1) eÅ^{-3} and 2·6(1) eÅ^{-5}, respectively. The fact that the differences are only marginal, indicates clearly that the aromatic character is not just limited to the naphthalene residue, but is spread over the central ring as well.

We found it instructive to examine the charge density distribution along the ring axis- the line perpendicular to the ring, passing through its RCP: as this would provide information on the spread of the π-electron cloud above and below the ring plane. Traversing a distance of 1 Å above and below each ring, we find distinct differences in

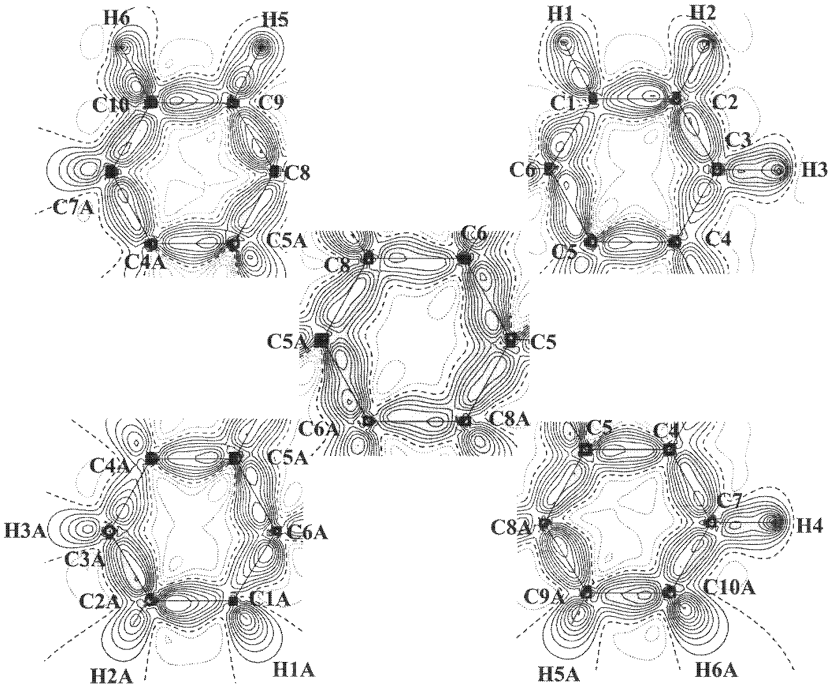

Figure 3. Static deformation density map of each ring. Contour intervals are given at 0·1 eÅ^{-3}.

Table 3. Charge density parameters of perylene – Bond critical point properties.

Bond	r_{BCP} (eÅ^{-3})	$\nabla^2 r_{BCP}$ (eÅ^{-5})	l_1 (eÅ^{-5})	l_2 (eÅ^{-5})	l_3 (eÅ^{-5})
C(1)–C(2)	2·12 (5)	−19·8 (1)	−18·74	−13·41	12·35
C(2)–C(3)	2·35 (5)	−23·5 (1)	−20·65	−15·61	12·74
C(3)–C(4)	1·88 (4)	−13·6 (1)	−15·16	−11·27	12·86
C(4)–C(5)	2·03 (4)	−15·0 (1)	−17·74	−11·17	13·95
C(5)–C(6)	2·08 (4)	−15·6 (1)	−18·77	−12·45	15·65
C(6)–C(1)	2·05 (5)	−18·6 (2)	−17·27	−13·05	11·68
C(6)–C(8)	1·80 (4)	−11·8 (1)	−15·17	−10·63	13·96
C(8)–C(9)	2·34 (5)	−23·8 (1)	−20·94	−15·61	12·76
C(9)–C(10)	2·10 (5)	−18·0 (1)	−18·06	−12·96	13·02
C(4)–C(7)	2·11 (4)	−16·7 (1)	−17·40	−12·99	13·70
C(7)–C(10A)	2·2 (7)	−22·1 (2)	−18·58	−15·80	12·33
C(10A)–C(9A)	2·08 (6)	−18·2 (1)	−18·15	−12·92	12·90
C(9A)–C(8A)	2·29 (6)	−24·0 (2)	−21·01	−15·48	12·52
C(8A)–C(5)	2·02 (6)	−17·0 (2)	−16·91	−13·24	13·14
C(8A)–C(6A)	1·76 (5)	−12·3 (1)	−15·24	−10·54	13·52
C(6A)–C(5A)	2·04 (5)	−16·0 (1)	−18·85	−12·35	15·16
C(5A)– C(4A)	2·00 (5)	−15·3 (1)	−17·79	−11·11	13·64
C(4A)–C(3A)	1·86 (6)	−13·9 (2)	−15·23	−11·22	12·59
C(3A)–C(2A)	2·34 (6)	−23·7 (2)	−20·69	−15·58	12·59
C(2A)–C(1A)	2·11 (6)	−19·9 (2)	−18·80	−13·37	12·26
C(1A)–C(6A)	2·04 (6)	−18·7 (2)	−17·30	−13·03	11·61
C(4A)–C(7A)	2·07 (6)	−17·1 (1)	−17·50	−12·90	13·26
C(7A)–C(10)	2·23 (8)	−21·8 (2)	−18·57	−15·77	12·52
C(7A)–H(4A)	1·79 (9)	−15·1 (3)	−18·34	−16·54	19·76
C(10)–H(6)	1·8 (1)	−14·4 (4)	−20·59	−17·61	23·81
C(9)–H(5)	1·70 (9)	−11·5 (3)	−18·18	−16·27	22·95
C(1)–H(1)	1·74 (8)	−12·7 (3)	−18·62	−16·48	22·42
C(2)–H(2)	1·89 (7)	−19·2 (2)	−19·80	−18·28	18·85
C(3)–H(3)	1·83 (7)	−15·5 (2)	−18·74	−16·07	19·31
C(7)–H(4)	1·79 (7)	−15·1 (2)	−18·28	−16·53	19·70
C(10A)–H(6A)	1·77 (9)	−14·4 (4)	−20·54	−17·58	23·72
C(9A)–H(5A)	1·72 (8)	−11·3 (3)	−18·26	−16·47	23·42
C(1A)–H(1A)	1·72 (9)	−12·8 (3)	−18·57	−16·33	22·11
C(2A)–H(2A)	1·89 (8)	−19·2 (2)	−19·80	−18·28	18·84
C(3A)–H(3A)	1·82 (8)	−15·6 (2)	−18·71	−15·98	19·12

the charge distribution between the naphthalene residues and the central *peri*-ring. Figure 4 depicts a plot of the Laplacian versus the distance, *d*, from the RCP. We see that the variation in the Laplacian is symmetrical across the ring plane for the central ring while for the naphthalene rings, the distribution is uneven. This is clearly understandable based on the geometry of the molecule. Negative values of *d* stand for the inside region of the bow-shaped molecule (see inset of figure 4) where, for the naphthalene residue, the $\boldsymbol{p}$ cloud from the neighbouring ring may show some overlap enhancing the Laplacian. In what follows, we have used data from the 'positive-*d*' region.

In figure 5, we have plotted Laplacian versus electron density above the ring plane. At all RCPs, the Laplacian is ~2·5 eÅ^{-5} with a density of 0·1 eÅ^{-3}, both decreasing gradually as one moves away from the ring plane. We see that the decrease in Laplacian with density is more steep for the central ring compared to the naphthalene rings, which is

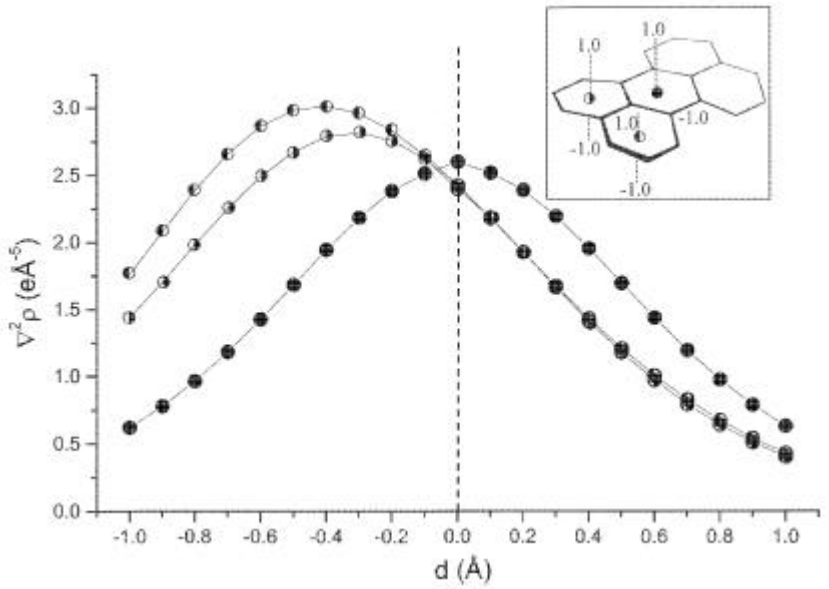

Figure 4. Variation of the Laplacian with distance, *d*, along the ring axis. The data points have been obtained at intervals of 0·1 Å up to 1 Å above and below the ring plane. The bow-shaped molecule is shown schematically in the inset.

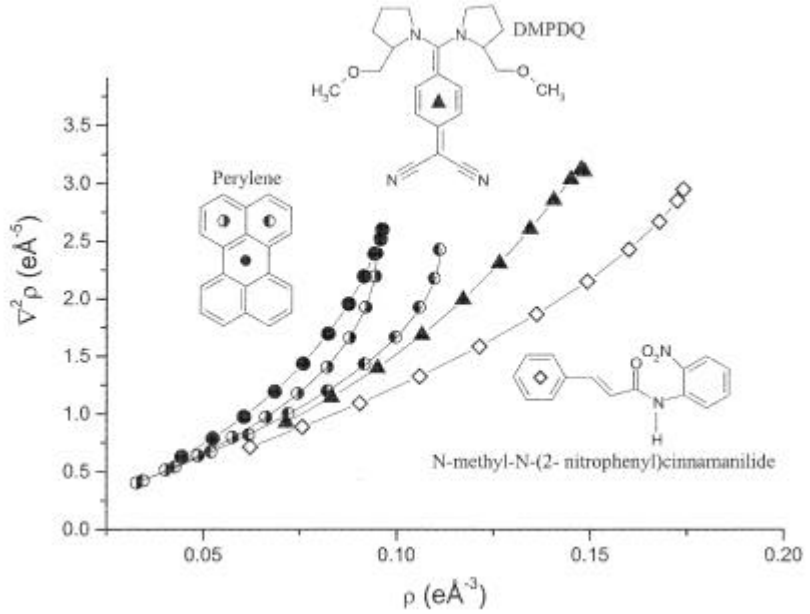

Figure 5. Variation of the Laplacian with the density along the ring axis. The data points have been obtained at intervals of 0·1 Å up to 1 Å above the ring plane. The structural diagrams of the molecules are shown adjacent to the curves along with the respective symbols.

indicative of a smeared p cloud in the former. In figure 5, we have also plotted Laplacian and density data from the quinoid ring of DMPDQ[12] and a regular phenyl ring from the cinnamanilide derivative.[13] The quinoid ring is known to have some benzenoid character, an effect arising from the charge polarisation from the functional groups in the molecule[12] and thus serves as another example of benzene-like rings in this study. The phenyl ring from cinnamanilide stands for a regular aromatic ring. We see from the figure that in both cases, the variation of Laplacian with density is much more gradual especially in the phenyl ring, when compared to perylene rings. Besides, the density and the Laplacian values are much higher. Thus, the plot in figure 5 brings out the extent of aromaticity associated with these rings, the central ring of perylene being the least aromatic. It is interesting to observe that the naphthalene residues no longer behave like phenyl rings due to the charge redistribution as a result of fusing.

4. Conclusions

The present study based on experimental charge density has brought out an understanding of aromaticity in fused phenyl rings of perylene in comparison to a quinoid ring and a regular phenyl ring. Topological analysis of the charge density at the bond- and ring critical points in perylene has shown that aromaticity is not just restricted to the naphthalene residues, but is smeared over the entire molecular surface. The Laplacian values below the bow-shaped naphthalene rings are relatively enhanced due to contributions from the neighbouring rings, while the variation is symmetric for the more-uniform central ring. A plot of the Laplacian versus density obtained at various points along the ring axis has provided a means of evaluating aromaticity in the various rings. As one moves away from the ring plane, the fall in the Laplacian along with density indicates how smeared is the p-density distribution. In the case of the regular phenyl ring of *N*-methyl-*N*-(2-nitrophenyl) cinnamanilide, the variation is shallow implying a well defined p-density over the ring region. For the benzene-like quinoid ring of DMPDQ and the naphthalene rings of perylene, the variation is increasingly steeper and reaches maximum for the central *peri*-ring. The latter is, therefore, considered pseudoaromatic.

Acknowledgement

The authors thank Professor C N R Rao, FRS for encouragement.

References

1. Gomes J A N F and Mallion R B 2001 *Chem. Rev.* **101** 1349
2. Mitchell R H 2001 *Chem. Rev.* **101** 1301
3. Julg A and Francois P H 1967 *Theor. Chem. Acta* **7** 249; Bird C W 1985 *Tetrahedron* **41** 1409; Schleyer P v R, Freeman P K, Jiao H and Goldfuss B 1995 *Angew. Chem., Int. Ed. Engl.* **34** 337
4. Dewar M J S and de Llano C 1969 *J. Am. Chem. Soc.* **91** 789
5. Klein D J 1989 *Pure Appl. Chem.* **61** 2107
6. Haigh C W and Mallion R B 1989 *Croat. Chem. Acta* **62** 1
7. Koritsanszky T S and Coppens P 2001 *Chem. Rev.* **101** 1583
8. Howard S T and Krygowski T M 1997 *Can. J. Chem.* **75** 1174
9. Ranganathan A and Kulkarni G U 2002 *J. Phys. Chem.* **A106** 7813
10. Farges J-P 1994 In *Organic conductors: Fundamentals and applications* (New York: Marcel Dekker)

11. Camerman A and Trotter J 1964 *Proc. R. Soc. London* **A279** 129
12. Gopalan R S, Kulkarni G U and Rao C N R 2001 *New J. Chem.* **25** 1108
13. Gopalan R S, Kulkarni G U, Subramanian E and Renganayaki S 2000 *J. Mol. Struct.* **524** 169
14. Tanaka J 1963 *Bull. Chem. Soc. Jpn.* **36** 1237
15. Hansen N K and Coppens P 1978 *Acta Crystallogr.* **A34** 909
16. Allen F H, Kennard O, Watson D G, Brammer L, Orpen A G and Taylor R 1987 *J. Chem. Soc., Perkin Trans. 2* S1
17. Koritsanszky T, Howard S T, Richter T, Mallinson P R, Su Z and Hansen N K 1995 XD, A computer program package for multipole refinement and analysis of charge densities from diffraction data, Cardiff, Glasgow, Buffalo, Nancy, Berlin
18. Hirshfeld F L 1976 *Acta Crystallogr.* **A32** 239
19. Dewar M J S and Schmeising H N 1959 *Tetrahedron* **5** 166